On the emergence of Raman signals characterizing multicenter nanoscale interactions

Mathew D. Williams, David S. Bradshaw and David L. Andrews*
School of Chemistry, University of East Anglia, Norwich NR4 7TJ, United Kingdom

ABSTRACT

Raman scattering is most commonly associated with a change in vibrational state within one molecule, with signals in the corresponding spectrum widely used to identify material structures. When the corresponding theory is developed using quantum electrodynamics, the fundamental scattering process is described by a single photon of one radiation mode being annihilated with the concurrent creation of another photon; the two photon energies differ by an amount corresponding to the transfer of vibrational energy within the system. Here, we consider nanoscale interactions between neighboring molecules to mediate the process, by way of a virtual photon exchange to connect the evolution of the two molecular states. We consider both a single and pair of virtual photon exchanges. Our analysis deploys two realistic assumptions: in each pairwise interaction the two components are considered to be (*i*) chemically different and (*ii*) held in a fixed orientation with respect to each other, displaced by an amount equivalent to the near-field region; resulting in higher order dependences on displacement R becoming increasingly significant, and at the limit the short-range R^{-6} term can even dominate over R^{-3} dependence. In our investigation one center undergoes a change in vibrational energy; each neighboring molecule returns to the electronic and vibrational state in which it began. For the purposes of providing results, a Stokes transition has been assumed; analogous principles hold for the anti-Stokes counterpart. Experimentally, there is no change to the dependence on the intensity of laser light. However, the various mechanisms presented herein lead to different selection rules applying in each instance. In some cases specifically identifiable mechanisms will be active for a given transition, leading to new and characteristic lines in the Raman spectrum. A thorough investigation of all physically achievable mechanisms will be detailed in this work.

Keywords: Raman spectroscopy, Molecular interactions, Inelastic scattering, Quantum electrodynamics, Nanophotonics, Virtual photon, Nanoparticle.

1. INTRODUCTION

Discovered in the 1920s, Raman (inelastic) scattering is a well-established process that typically involves a single optical center.[1] It is presently used as both a spectroscopic[2-4] and microscopic[5-6] tool. Moreover, techniques such as surface-enhanced Raman scattering[7-12] are becoming increasingly prominent. The theory of Raman scattering is well-known with quantum electrodynamics (QED) offering the most accurate and insightful means of formulation.[13] In such a framework, Raman scattering involves the concurrent annihilation and creation of photons with two different radiation modes and non-equivalent energies, this difference a resulting from a change in vibrational state of the molecule (optical center). Although Raman scattering usually involves individual optical centers, this work investigates the influence of a neighboring molecule in close proximity; this research is beyond the familiar heterogeneous broadening of spectral lines. In the presented scenarios, the coupling between optical centers is mediated by one or two virtual photon exchanges,[14-16] which may lead to different selection rules and indeed explanations for previously overlooked characteristic lines on the Raman spectrum.

The following analysis of Raman scattering at an optical center under the influence of a neighbor involves two realistic assumptions: the components are chemically different, and held in a fixed orientation with respect to each other in the near-zone region. Due to the latter, each virtual photon exchange can justifiably be represented by a short-range dipole-dipole coupling tensor. For optical centers separated by a few nanometers, the higher order dependences on displacement R

become increasingly significant and they are more likely to be experimentally measurable. In the interaction of interest, one of the optical centers will undergo a change in vibrational energy (*i.e.* a Raman transition) while the neighboring center will remain an identical state before and after the process. Here, a Stokes transition is assumed, although analogous principles hold for the anti-Stokes counterpart. The following section details the well-established theory for Raman scattering, the two sections that follow accommodate the neighboring center. The paper then concludes with a discussion.

2. SINGLE-CENTER RAMAN SCATTERING

The following analysis uses quantum electrodynamics, in this framework both the molecular and radiation states are quantized and a series of Feynman diagrams offer a visualization of the process.[13] In the case of the fundamental (single-center) Raman scattering, the molecule begins in the ground state and undergoes concurrent photon annihilation and creation events each of a different radiation mode – the change in photonic energy is transferred to the molecule in the form of an excitation of a vibrational mode (see Figure 1). Such a mechanism can be represented mathematically by a matrix element, from which an expression relating to an observable can be produced via Fermi's golden rule.[17] The matrix element, M_{FI}, for Raman scattering is given by;

$$M_{FI} = -\bar{e}_i' e_j \alpha_{ij}^{\alpha 0} . \tag{1}$$

Here, the superscripts 0 and α represent the ground and final molecular states, respectively, **e** is the polarization of the electric field of the incident (annihilated) light, with the overbar denoting its complex conjugate and the inclusion of the prime denotes scattered (created) light. The transition polarizability, $\alpha_{ij}^{\alpha 0}$, is written explicitly as;

$$\alpha_{ij}^{\alpha 0} = \sum_r \left\{ \frac{\mu_i^{\alpha r} \mu_j^{r0}}{E_{r0} - \hbar ck} + \frac{\mu_i^{\alpha r} \mu_j^{r0}}{E_{r0} + \hbar ck'} \right\}, \tag{2}$$

which involves a summation over the virtual intermediate states, r. In this expression, each $\boldsymbol{\mu}$ denotes a transition dipole moments, $\hbar ck$ and $\hbar ck'$ are the energies of the incident and scattered photon, respectively, and the difference in molecular state energies are given by $E_\alpha - E_0 \equiv E_{\alpha 0} = \hbar ck - \hbar ck'$.

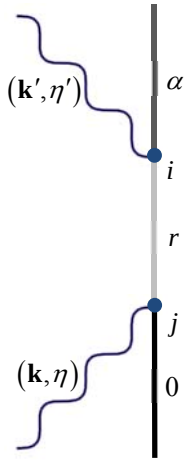

Figure 1. One of two Feynman diagrams for single center Raman scattering. From the bottom upwards: a photon of wavevector **k** and polarization η is annihilated; at this point the molecule enters a virtual intermediate state r; in the following instant a photon of different wavevector **k′** and polarization η' are created. The overall change in energy of the radiation field is equivalent to a change in energy of the molecular states $E_\alpha - E_0$, where α relates to a vibrational excitation (rather than electronic) and 0 denotes a ground state.

3. TWO-CENTER RAMAN SCATTERING

A. One virtual photon exchange

In the following it is assumed that the optical center *A* is the one that undergoes the Raman transition. To accommodate the influence of the neighboring center *B*, a molecule that begins and ends in the same state, an expression for the radiant intensity (which is dependent on the solid angle Ω′) is found using;

$$I'(\Omega') = \left(\frac{k'^2}{4\pi\varepsilon_0}\right)^2 I_0 \left| M_{FI}^{A'|B} + M_{FI}^{B'|A} + M_{FI}^{A|B'} + M_{FI}^{B|A'} + M_{FI}^{A'\|B} + M_{FI}^{B'\|A} + M_{FI}^{A\|B'} + M_{FI}^{B\|A'} \right|^2 . \tag{3}$$

Here, I_0 is the intensity of the input beam and the superscripts represent the optical centers with the convention: the first symbol (read left-to-right) denotes the site of absorption, the number of solidi signifies the number (either one or two) of virtual photons exchanged, and the prime represents the optical center that creates a photon. All these contributions involve the same number of detectable (real) photons and, therefore, all have the same linear dependence on radiant intensity. Each of the eight terms in equation (3) represents a different process, all of them are considered in the following text.

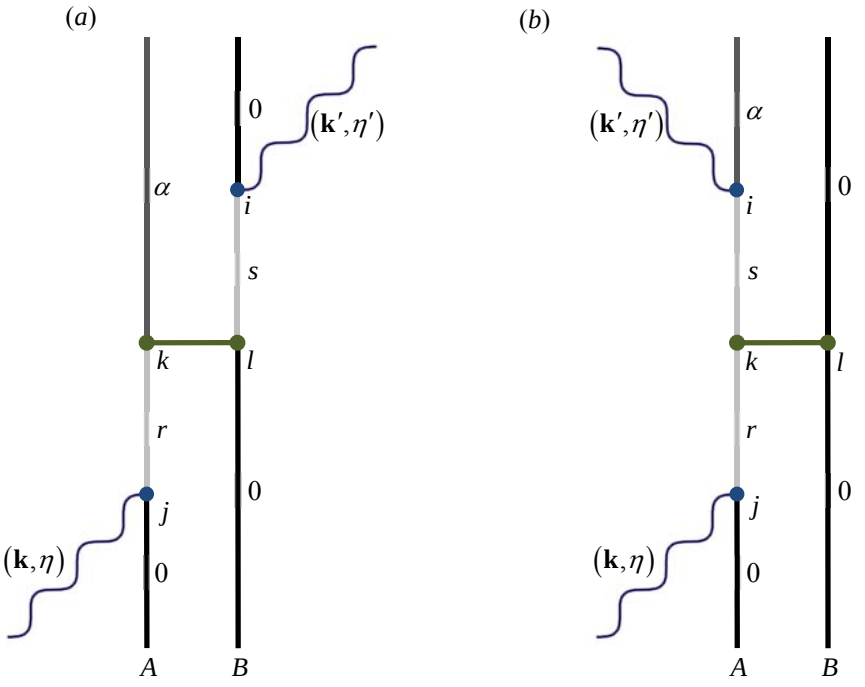

Figure 2. Representative Feynman diagrams for two-center Raman scattering, where the optical centers *A* and *B* are coupled together by a single virtual photon: (*a*) two interactions occur at each site; (*b*) three interactions at *A* and one at *B*. The horizontal line depicts near-zone exchange, and *r* and *s* denote virtual intermediate states.

The set of four that involve a single virtual photon exchange between the two molecules are first examined, which include: (*i*) photon annihilation at *A* and photon creation at *B*, denoted by $M_{FI}^{A|B'}$ and shown in Figure 2(*a*); (*ii*) annihilation at *B* and creation at *A*, signified by $M_{FI}^{B|A'}$; (*iii*) photon annihilation and creation at *A*, represented by $M_{FI}^{A'|B}$ and given in Figure 2(*b*), and; (*iv*) annihilation and creation at *B*, symbolized by $M_{FI}^{B'|A}$. The even-numbered cases can be readily adapted from their odd numbered counterparts displayed above. Each of the cases (*i*) through (*iv*) has six possible

variations in the time-ordering of the interaction events. In the near-zone region, the matrix elements corresponding to the first two respective cases are written in the form:

$$M_{FI}^{A|B'} = \frac{1}{4\pi\varepsilon_0 R^3}\bar{e}_i' e_j \left(\delta_{kl} - 3\hat{R}_k\hat{R}_l\right)\alpha_{jk}'^{\alpha 0|A}\alpha_{il}''^{00|B}, \tag{4}$$

$$M_{FI}^{B|A'} = \frac{1}{4\pi\varepsilon_0 R^3}\bar{e}_i' e_j \left(\delta_{kl} - 3\hat{R}_k\hat{R}_l\right)\alpha_{jk}'^{00|B}\alpha_{il}''^{\alpha 0|A}, \tag{5}$$

where the short-range coupling tensor **V** has been directly employed[14] and the explicit form of the individual polarizability tensors, relating to the separate forms of two-photon interaction at either molecule, are given by;

$$\alpha_{jk}'^{\alpha 0|A} = 2\sum_r \left\{\frac{\mu_k^{\alpha r|A}\mu_j^{r0|A}}{E_{r0}^A - \hbar ck} + \frac{\mu_j^{\alpha r|A}\mu_k^{r0|A}}{E_{r0}^A + \hbar ck'}\right\}, \tag{6}$$

$$\alpha_{il}''^{00|B} = 2\sum_s \left\{\frac{\mu_i^{0s|B}\mu_l^{s0|B}}{E_{s0}^B - \hbar ck'} + \frac{\mu_l^{0s|B}\mu_i^{s0|B}}{E_{s0}^B + \hbar ck'}\right\}. \tag{7}$$

Cases (*iii*) and (*iv*) involve a three-photon interaction at one molecule and a single interaction at the other, so that the respective tensors β_{ijk} (hyperpolarizability form) and μ_l (dipole) are employed, to obtain;

$$M_{FI}^{A'|B} = \frac{1}{4\pi\varepsilon_0 R^3}\bar{e}_i' e_j \left(\delta_{kl} - 3\hat{R}_k\hat{R}_l\right)\beta_{ijk}^{\alpha 0|A}\mu_l^{00|B}, \tag{8}$$

$$M_{FI}^{B'|A} = \frac{1}{4\pi\varepsilon_0 R^3}\bar{e}_i' e_j \left(\delta_{kl} - 3\hat{R}_k\hat{R}_l\right)\beta_{ijk}^{00|B}\mu_l^{\alpha 0|A}. \tag{9}$$

Here, in the former, $\mu_l^{00|B}$ denotes a permanent static dipole and the explicit form of the transition hyperpolarizability is given by;

$$\begin{aligned}\beta_{ijk}^{\alpha 0|A} = \sum_{r,s}\Bigg\{&\frac{\mu_i^{\alpha s|A}\mu_k^{sr|A}\mu_j^{r0|A}}{\left(E_{s0}^A - \hbar ck\right)\left(E_{r0}^A - \hbar ck\right)} + \frac{\mu_k^{\alpha s|A}\mu_i^{sr|A}\mu_j^{r0|A}}{E_{s\alpha}^A\left(E_{r0}^A - \hbar ck\right)} + \frac{\mu_i^{\alpha s|A}\mu_j^{sr|A}\mu_k^{r0|A}}{E_{r0}^A\left(E_{s0}^A - \hbar ck\right)} \\ &+ \frac{\mu_k^{\alpha s|A}\mu_j^{sr|A}\mu_i^{r0|A}}{E_{s\alpha}^A\left(E_{r0}^A + \hbar ck'\right)} + \frac{\mu_j^{\alpha s|A}\mu_i^{sr|A}\mu_k^{r0|A}}{E_{r0}^A\left(E_{s0}^A + \hbar ck'\right)} + \frac{\mu_j^{\alpha s|A}\mu_k^{sr|A}\mu_i^{r0|A}}{\left(E_{s0}^A + \hbar ck'\right)\left(E_{r0}^A + \hbar ck'\right)}\Bigg\}.\end{aligned} \tag{10}$$

Since mechanisms (*iii*) and (*iv*) involve a tensor of the above form, the corresponding selection rules relate to three-photon processes, such as hyper-Raman scattering. Therefore, the allowed irreducible representations are those under which cubic functions naturally transform. These can be found in more detailed character tables.[18]

B. Two-virtual photon exchange

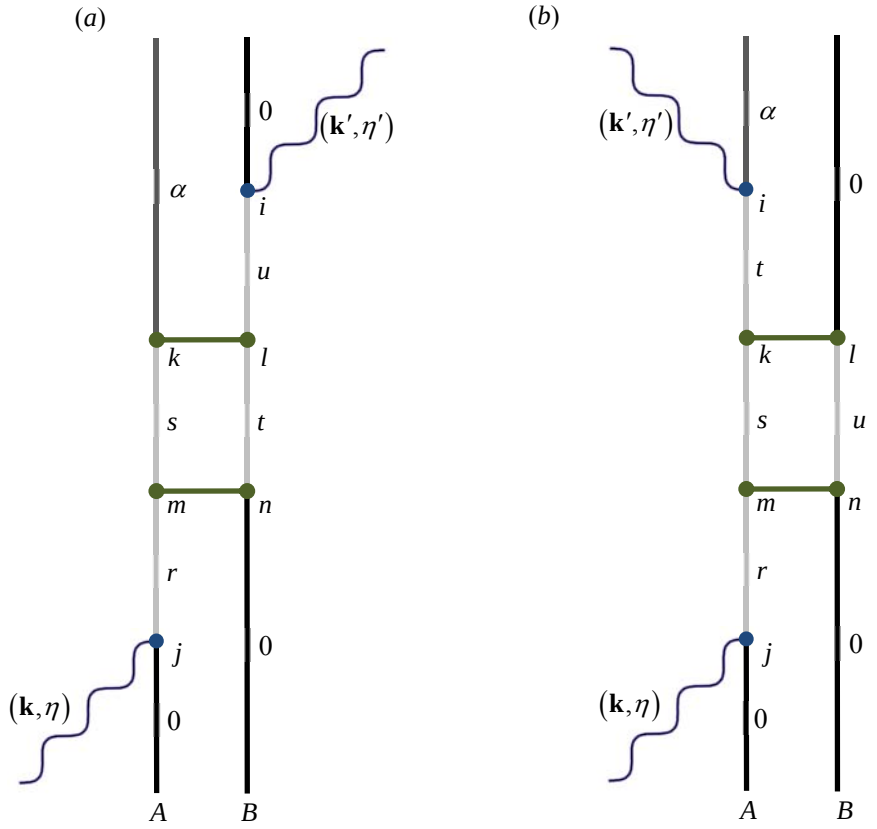

Figure 3. Same as Figure 2, except two virtual photon exchanges occur between molecules *A* and *B*, namely: (*a*) three interactions at *A* and one at *B*; (*b*) two interactions at each site. Additional intermediary state, *t* and *u*, are assigned to either molecule.

Now consider the second set of four processes, i.e. those that involve two virtual photons. In sequence, the cases (*v*)-(*viii*) are identical to the first set (*i*)-(*iv*) – except for the inclusion of a second virtual photon coupling; each mechanism has twelve possible permutations. Figures 3(*a*) and (*b*) depict indicative Feynman diagrams for cases (*v*) and (*vii*), respectively, and correspond to $M_{FI}^{A\|B'}$ and $M_{FI}^{A'\|B}$. Again, each Feynman diagram above can be intuitively redrawn to represent cases (*vi*) and (*viii*). In the near-zone region, the matrix elements that correspond to cases (*v*) and (*vi*) are written as:

$$M_{FI}^{A'\|B} = -\left(\frac{1}{4\pi\varepsilon_0 R^3}\right)^2 \bar{e}_i' e_j \left(\delta_{kl} - 3\hat{R}_k\hat{R}_l\right)\left(\delta_{mn} - 3\hat{R}_m\hat{R}_n\right)\chi_{ijkm;ln}^{\alpha 0|A;00|B}, \tag{11}$$

$$M_{FI}^{B'\|A} = -\left(\frac{1}{4\pi\varepsilon_0 R^3}\right)^2 \bar{e}_i' e_j \left(\delta_{kl} - 3\hat{R}_k\hat{R}_l\right)\left(\delta_{mn} - 3\hat{R}_m\hat{R}_n\right)\chi_{ijkm;ln}^{00|B;\alpha 0|A}. \tag{12}$$

Here, since additional complexities arise due to the second virtual photon, the χ tensors cannot be split into two and assigned to molecules *A* and *B*. Therefore, the χ tensors involve a mixture of features from both molecules: one such tensor is written explicitly as;

$$\chi^{\alpha 0|A;00|B}_{ijkm;ln} = \sum_{r,s,t,u}\left\{\frac{\mu_i^{\alpha t|A}\mu_k^{ts|A}\mu_m^{sr|A}\mu_j^{r0|A}\mu_l^{0u|B}\mu_n^{u0|B}}{\left(E^A_{t0}-\hbar ck\right)\left(E^A_{s0}+E^B_{u0}-\hbar ck\right)\left(E^A_{r0}-\hbar ck\right)}+\frac{\mu_k^{\alpha t|A}\mu_i^{ts|A}\mu_m^{sr|A}\mu_j^{r0|A}\mu_l^{0u|B}\mu_n^{u0|B}}{\left(E^A_{t\alpha}+E^B_{u0}\right)\left(E^A_{s0}+E^B_{u0}-\hbar ck\right)\left(E^A_{r0}-\hbar ck\right)}\right.$$
$$+\frac{\mu_k^{\alpha t|A}\mu_m^{ts|A}\mu_i^{sr|A}\mu_j^{r0|A}\mu_l^{0u|B}\mu_n^{u0|B}}{E^A_{s\alpha}\left(E^A_{t\alpha}+E^B_{u0}\right)\left(E^A_{r0}-\hbar ck\right)}+\frac{\mu_i^{\alpha t|A}\mu_k^{ts|A}\mu_j^{sr|A}\mu_m^{r0|A}\mu_l^{0u|B}\mu_n^{u0|B}}{\left(E^A_{t0}-\hbar ck\right)\left(E^A_{s0}+E^B_{u0}-\hbar ck\right)\left(E^A_{r0}+E^B_{u0}\right)}$$
$$+\frac{\mu_k^{\alpha t|A}\mu_i^{ts|A}\mu_j^{sr|A}\mu_m^{r0|A}\mu_l^{0u|B}\mu_n^{u0|B}}{\left(E^A_{t\alpha}+E^B_{u0}\right)\left(E^A_{s0}+E^B_{u0}-\hbar ck\right)\left(E^A_{r0}+E^B_{u0}\right)}+\frac{\mu_k^{\alpha t|A}\mu_m^{ts|A}\mu_j^{sr|A}\mu_i^{r0|A}\mu_l^{0u|B}\mu_n^{u0|B}}{E^A_{s\alpha}\left(E^A_{t\alpha}+E^B_{u0}\right)\left(E^A_{r0}+\hbar ck'\right)}$$
$$+\frac{\mu_i^{\alpha t|A}\mu_j^{ts|A}\mu_k^{sr|A}\mu_m^{r0|A}\mu_l^{0u|B}\mu_n^{u0|B}}{E^A_{s0}\left(E^A_{t0}-\hbar ck\right)\left(E^A_{r0}+E^B_{0u}\right)}+\frac{\mu_k^{\alpha t|A}\mu_j^{ts|A}\mu_i^{sr|A}\mu_m^{r0|A}\mu_l^{0u|B}\mu_n^{u0|B}}{\left(E^A_{t\alpha}+E^B_{u0}\right)\left(E^A_{s0}+E^B_{u0}+\hbar ck'\right)\left(E^A_{r0}+E^B_{u0}\right)}$$
$$+\frac{\mu_k^{\alpha t|A}\mu_j^{ts|A}\mu_m^{sr|A}\mu_i^{r0|A}\mu_l^{0u|B}\mu_n^{u0|B}}{\left(E^A_{t\alpha}+E^B_{u0}\right)\left(E^A_{s0}+E^B_{u0}+\hbar ck'\right)\left(E^A_{r0}+\hbar ck'\right)}+\frac{\mu_j^{\alpha t|A}\mu_i^{ts|A}\mu_k^{sr|A}\mu_m^{r0|A}\mu_l^{0u|B}\mu_n^{u0|B}}{E^A_{s0}\left(E^A_{t0}+\hbar ck'\right)\left(E^A_{r0}+E^B_{u0}\right)}$$
$$\left.+\frac{\mu_j^{\alpha t|A}\mu_k^{ts|A}\mu_i^{sr|A}\mu_m^{r0|A}\mu_l^{0u|B}\mu_n^{u0|B}}{\left(E^A_{t0}+\hbar ck'\right)\left(E^A_{s0}+E^B_{u0}+\hbar ck'\right)\left(E^A_{r0}+E^B_{u0}\right)}+\frac{\mu_j^{\alpha t|A}\mu_k^{ts|A}\mu_m^{sr|A}\mu_i^{r0|A}\mu_l^{0u|B}\mu_n^{u0|B}}{\left(E^A_{t0}+\hbar ck'\right)\left(E^A_{s0}+E^B_{u0}+\hbar ck'\right)\left(E^A_{r0}+\hbar ck'\right)}\right\}. \quad (13)$$

Evidently it is impossible to fully separate individual terms with dependences on molecules *A* and *B* in this equation; however, the selection rules and symmetry arguments can be applied to the numerators (each of which can be thus decomposed). Since the latter all involve four dipole moments on molecule *A* and two on *B*, it is legitimate to relate *A* to the four-photon selection rules and *B* to two-photon rules. The expression for cases (*vii*) and (*viii*) are given by;

$$M_{FI}^{A\|B'} = -\left(\frac{1}{4\pi\varepsilon_0 R^3}\right)^2 \bar{e}_i' e_j \left(\delta_{kl}-3\hat{R}_k\hat{R}_l\right)\left(\delta_{mn}-3\hat{R}_m\hat{R}_n\right)\chi'^{\alpha 0|A;00|B}_{jkm;iln}, \quad (14)$$

$$M_{FI}^{B\|A'} = -\left(\frac{1}{4\pi\varepsilon_0 R^3}\right)^2 \bar{e}_i' e_j \left(\delta_{kl}-3\hat{R}_k\hat{R}_l\right)\left(\delta_{mn}-3\hat{R}_m\hat{R}_n\right)\chi'^{00|B;\alpha 0|A}_{jkm;iln}, \quad (15)$$

with the molecular response tensor, corresponding to equation (14), written as:

$$\chi'^{\alpha 0|A;00|B}_{jkm;iln} = \sum_{r,s,t,u}\left\{\frac{\mu_k^{\alpha s|A}\mu_m^{sr|A}\mu_j^{r0|A}\mu_i^{0u|B}\mu_l^{ut|B}\mu_n^{t0|B}}{\left(E^B_{u0}-\hbar ck'\right)\left(E^A_{s0}+E^B_{t0}-\hbar ck\right)\left(E^A_{r0}-\hbar ck\right)}+\frac{\mu_k^{\alpha s|A}\mu_m^{sr|A}\mu_j^{r0|A}\mu_l^{0u|B}\mu_i^{ut|B}\mu_n^{t0|B}}{\left(E^A_{s\alpha}+E^B_{u0}\right)\left(E^A_{s0}+E^B_{t0}-\hbar ck\right)\left(E^A_{r0}-\hbar ck\right)}\right.$$
$$+\frac{\mu_k^{\alpha s|A}\mu_m^{sr|A}\mu_j^{r0|A}\mu_l^{0u|B}\mu_n^{ut|B}\mu_i^{t0|B}}{\left(E^A_{s\alpha}+E^B_{u0}\right)\left(E^A_{r\alpha}+E^B_{t0}\right)\left(E^A_{r0}-\hbar ck\right)}+\frac{\mu_k^{\alpha s|A}\mu_j^{sr|A}\mu_m^{r0|A}\mu_l^{0u|B}\mu_i^{ut|B}\mu_n^{t0|B}}{\left(E^B_{u0}-\hbar ck'\right)\left(E^A_{s0}+E^B_{t0}-\hbar ck\right)\left(E^A_{r0}+E^B_{t0}\right)}$$
$$+\frac{\mu_k^{\alpha s|A}\mu_j^{sr|A}\mu_m^{r0|A}\mu_l^{0u|B}\mu_i^{ut|B}\mu_n^{t0|B}}{\left(E^A_{s\alpha}+E^B_{u0}\right)\left(E^A_{s0}+E^B_{t0}-\hbar ck\right)\left(E^A_{r0}+E^B_{t0}\right)}+\frac{\mu_k^{\alpha s|A}\mu_m^{sr|A}\mu_j^{r0|A}\mu_l^{0u|B}\mu_n^{ut|B}\mu_i^{t0|B}}{\left(E^A_{s\alpha}+E^B_{u0}\right)\left(E^A_{r\alpha}+E^B_{t0}\right)\left(E^B_{t0}+\hbar ck'\right)}$$
$$+\frac{\mu_j^{\alpha s|A}\mu_k^{sr|A}\mu_m^{r0|A}\mu_i^{0u|B}\mu_l^{ut|B}\mu_n^{t0|B}}{\left(E^B_{u0}-\hbar ck'\right)\left(E^A_{s0}+E^B_{u0}\right)\left(E^A_{r0}+E^B_{t0}\right)}+\frac{\mu_k^{\alpha s|A}\mu_j^{sr|A}\mu_m^{r0|A}\mu_l^{0u|B}\mu_i^{ut|B}\mu_n^{t0|B}}{\left(E^A_{s\alpha}+E^B_{u0}\right)\left(E^A_{r0}+E^B_{u0}+\hbar ck'\right)\left(E^A_{r0}+E^B_{t0}\right)}$$
$$+\frac{\mu_k^{\alpha s|A}\mu_j^{sr|A}\mu_m^{r0|A}\mu_l^{0u|B}\mu_n^{ut|B}\mu_i^{t0|B}}{\left(E^A_{s\alpha}+E^B_{u0}\right)\left(E^A_{r0}+E^B_{u0}+\hbar ck'\right)\left(E^B_{t0}+\hbar ck'\right)}+\frac{\mu_j^{\alpha s|A}\mu_k^{sr|A}\mu_m^{r0|A}\mu_l^{0u|B}\mu_i^{ut|B}\mu_n^{t0|B}}{\left(E^A_{s0}+\hbar ck'\right)\left(E^A_{s0}+E^B_{u0}\right)\left(E^A_{r0}+E^B_{t0}\right)}$$
$$\left.+\frac{\mu_j^{\alpha s|A}\mu_k^{sr|A}\mu_m^{r0|A}\mu_l^{0u|B}\mu_n^{ut|B}\mu_i^{t0|B}}{\left(E^A_{s0}+\hbar ck'\right)\left(E^A_{r0}+E^B_{u0}+\hbar ck'\right)\left(E^B_{t0}+\hbar ck'\right)}+\frac{\mu_j^{\alpha s|A}\mu_k^{sr|A}\mu_m^{r0|A}\mu_l^{0u|B}\mu_n^{ut|B}\mu_i^{t0|B}}{\left(E^A_{s0}+\hbar ck'\right)\left(E^A_{r0}+E^B_{u0}+\hbar ck'\right)\left(E^B_{t0}+\hbar ck'\right)}\right\}. \quad (16)$$

4. DISCUSSION

In this work we have investigated systems in which a Raman spectrum, most commonly interpreted in terms of vibrations within individual molecules, can be modified as a result of nanoscale interactions between neighboring molecules. Using a quantum electrodynamical development of theory the analysis has focused on twin-component chemical systems within which molecular pairs are held at short range in a fixed orientation. It emerges that the Raman quantum amplitude contains additional terms with R^{-3} and R^{-6} dependences on the molecular separation R, leading to Raman line intensities ranging from R^{-3} to R^{-12}. The various mechanisms that can participate lead to variations in the selection rules, and in certain cases characteristic new lines in the Raman spectrum. Having now identified the electrodynamic mechanisms, and ascertained the practicability of detection, this analysis now paves the way for a more thorough investigation of the detailed, corresponding selection rules.

ACKNOWLEDGEMENTS

We thank the University of East Anglia (UEA) and the Engineering and Physical Sciences Research Council (EPSRC) for funding this research. We are grateful to Dr. Juan Rodriguez Ruiz (Universidad de Málaga), a visiting scholar at UEA, for his insightful comments.

REFERENCES

[1] Long, D. A., [The Raman effect: a unified treatment of the theory of Raman scattering by molecules], Wiley, Chichester; New York (2002).
[2] Chrimes, A. F., Khoshmanesh, K., Stoddart, P. R., Mitchell, A. and Kalantar-zadeh, K., "Microfluidics and Raman microscopy: current applications and future challenges," Chem. Soc. Rev. 42, 5880-5906 (2013).
[3] Palonpon, A. F., Sodeoka, M. and Fujita, K., "Molecular imaging of live cells by Raman microscopy," Curr. Opin. Chem. Biol. 17, 708-715 (2013).
[4] Antonio, K. A. and Schultz, Z. D., "Advances in Biomedical Raman Microscopy," Anal. Chem. 86, 30-46 (2014).
[5] Das, R. S. and Agrawal, Y. K., "Raman spectroscopy: Recent advancements, techniques and applications," Vib. Spectrosc 57, 163-176 (2011).
[6] Krafft, C. and Popp, J., "The many facets of Raman spectroscopy for biomedical analysis," Anal. Bioanal. Chem. 407, 699-717 (2014).
[7] Cialla, D., März, A., Böhme, R., Theil, F., Weber, K., Schmitt, M. and Popp, J., "Surface-enhanced Raman spectroscopy (SERS): progress and trends," Anal. Bioanal. Chem. 403, 27-54 (2011).
[8] Ru, E. C. L. and Etchegoin, P. G., "Single-Molecule Surface-Enhanced Raman Spectroscopy," Annu. Rev. Phys. Chem. 63, 65-87 (2012).
[9] Kim, Z. H., "Single-molecule surface-enhanced Raman scattering: Current status and future perspective," Frontiers of Physics 9, 25-30 (2013).
[10] Schlücker, S., "Surface-Enhanced Raman Spectroscopy: Concepts and Chemical Applications," Angew. Chem. Int. Ed. 53, 4756-4795 (2014).
[11] Yamamoto, Y. S., Ozaki, Y. and Itoh, T., "Recent progress and frontiers in the electromagnetic mechanism of surface-enhanced Raman scattering," J. Photochem. Photobiol. C 21, 81-104 (2014).
[12] Keller, E. L., Brandt, N. C., Cassabaum, A. A. and Frontiera, R. R., "Ultrafast surface-enhanced Raman spectroscopy," Analyst 140, 4922-4931 (2015).
[13] Craig, D. P. and Thirunamachandran, T., [Molecular Quantum Electrodynamics: An Introduction to Radiation-Molecule Interactions], Dover Publications, Mineola, NY (1998).
[14] Andrews, D. L. and Bradshaw, D. S., "Virtual photons, dipole fields and energy transfer: a quantum electrodynamical approach," Eur. J. Phys. 25, 845-858 (2004).
[15] Salam, A., [Molecular Quantum Electrodynamics: Long-Range Intermolecular Interactions], Wiley, Hoboken, NJ (2010).

[16] Andrews, D. L. and Bradshaw, D. S., "The role of virtual photons in nanoscale photonics," Ann. Phys. (Berlin) 526, 173-186 (2014).
[17] Mandel, L. and Wolf, E., [Optical Coherence and Quantum Optics], Cambridge University Press, Cambridge, NY, 871 (1995).
[18] Salthouse, J. A. and Ware, M. J., [Point Group Character Tables and Related Data], Cambridge University Press, London (1972).

*david.andrews@physics.org